

Historical effects of El Nino and La Nina events on the seasonal evolution of the montane snowpack in the Columbia and Colorado River Basins

Martyn P. Clark and Mark C. Serreze

Cooperative Institute for Research in Environmental Sciences, University of Colorado, Boulder, Colorado

Greg J. McCabe

U.S. Geological Survey, Lakewood, Colorado

Abstract. Snow-water equivalent (SWE) data measured at several hundred montane sites in the western United States are used to examine the historic effects of El Nino and La Nina events on seasonal snowpack evolution in the major subbasins in the Columbia and Colorado River systems. Results are used to predict annual runoff. In the Columbia River Basin, there is a general tendency for decreased SWE during El Nino years and increased SWE in La Nina years. However, the SWE anomalies for El Nino years are much less pronounced. This occurs in part because midlatitude circulation anomalies in El Nino years are located 35° east of those in La Nina years. This eastward shift is most evident in midwinter, at which time, SWE anomalies associated with El Nino are actually positive in coastal regions of the Columbia River Basin. In the Colorado River Basin, mean anomalies in SWE and annual runoff during El Nino years depict a transition between drier-than-average conditions in the north, and wetter-than-average conditions in the southwest. Associations during La Nina years are generally opposite those in El Nino years. SWE anomalies tend to be more pronounced in spring in the Lower Colorado River Basin. Our predictions of runoff reveal modest skill for scenarios using only historic El Nino and La Nina information. Predictions based on the water stored in the seasonal snowpack are, in almost all cases, much higher than those based on El Nino-Southern Oscillation (ENSO) information alone. However, combining observed midwinter snow conditions with information on seasonal snowpack evolution associated with ENSO improves predictions for basins in which ENSO signals exhibit strong seasonality.

1. Introduction

Variability in water resources over the western United States has numerous socio-economic impacts. Annual water consumption in the semiarid western United States averages 44% of renewable supplies, compared with 4% in the rest of the country [*el-Ashry and Gibbons, 1988*]. In the Colorado River Basin and southern California, groundwater is being mined and water supplies are being imported from adjoining states. Trade-offs among urban, agricultural, and environmental water needs have increased electricity transfers between the northwest and southwest regions during their respective peak and low periods [*Pulwarty and Redmond, 1997*]. The U.S. Bureau of Reclamation has indicated that during a dry period such as occurred from 1931–1940 the current water needs of the lower Colorado River Basin would not be met [*el-Ashry and Gibbons, 1988*]. In terms of flood hazard the severe flooding of the lower Colorado River Basin in spring 1983 resulted in \$80 million of economic losses [*Rhodes et al., 1984*]. Management of water in the western United States hence represents a formidable challenge. Managers must retain as much water as possible in reservoirs to meet the needs of irrigation, hydropower generation, domestic consumption, and recreation,

while still providing space in the reservoirs to protect downstream farms, homes, and businesses from flooding.

Of fundamental importance in developing water management strategies is knowledge of the state of the spring snowpack and its variability. In the montane regions of the western United States, between 50% and 70% of the annual precipitation falls as snow [*Serreze et al., 1999*] and is largely stored through the winter season. Knowledge of the water equivalent of the spring (e.g., April 1) snowpack can thus provide a useful approximation of annual runoff. This source of predictability was recognized early this century. Measurements of the seasonal snowpack in California began in the 1910s, and became much more widespread in the late 1930s, partly in response to the western drought of 1934.

The past decade has seen growing interest in understanding large-scale precipitation and temperature signals associated with the El Nino–Southern Oscillation (ENSO) [*Cayan and Peterson, 1990; Koch et al., 1991; Redmond and Koch, 1991; Cayan, 1996; McCabe and Dettinger, 1999; Wolter et al., 1999*]. This interest stems from the knowledge that El Nino and La Nina conditions are persistent and that their onset can be predicted several months in advance. El Nino (warm) events are characterized by above normal sea surface temperatures (SSTs) in the eastern tropical Pacific Ocean and increased tropical convection and precipitation near and east of the date line. During La Nina (cold) events, SST anomalies generally

Copyright 2001 by the American Geophysical Union.

Paper number 2000WR900305.
0043-1397/01/2000WR900305\$09.00

oppose those in El Niño events, but the negative anomalies in tropical convection and precipitation are smaller in magnitude and do not extend as far east [Hoerling *et al.*, 1997]. These tropical anomalies perturb the atmospheric circulation in mid-latitudes. In warm events the enhanced tropical convection results in intensification of the Hadley circulation and a strengthening and eastward extension of the Pacific subtropical jet. This is accompanied by deepening of the Aleutian Low in the North Pacific Ocean and amplification of the northward branch of the tropospheric wave train over North America, resulting in a characteristic “split flow” [e.g., Bjerknes, 1969; Horel and Wallace, 1981; Rasmusson and Wallace, 1983]. The midlatitude response to cold events is generally characterized by weakening of the subtropical jet and dampening of the wave train over North America. However, owing to the lack of symmetry in tropical convection patterns between warm and cold events, sea level pressure and 500 hPa height anomalies during warm events are shifted, on average, 35° east of those in cold events [Hoerling *et al.*, 1997].

In an analysis of hydrologic impacts of ENSO over the western United States, Cayan and Webb [1992] computed correlations between the Southern Oscillation index (SOI) (a simple measure of the phase/strength of ENSO) and April 1 snow-water equivalent (SWE) and between the SOI and annual runoff. They showed SWE and annual runoff to be positively correlated with the SOI in the northwestern United States but negatively correlated with the SOI in the southwestern United States. This suggests that El Niño (La Niña) events lead to decreased (increased) SWE and annual runoff in the northwest, and increased (decreased) SWE and annual runoff in the southwest. Other studies provide similar findings [Cayan and Peterson, 1990; Koch *et al.*, 1991; Redmond and Koch, 1991; Cayan, 1996]. These results reflect the perturbations in atmospheric circulation described earlier. In El Niño years the amplified northern branch of the wave train over North America is associated with higher temperatures over the northwestern United States and Canada, and tends to deflect storm systems northward toward Alaska, decreasing mean precipitation over the Pacific Northwest. Farther south, the strengthened subtropical jet entrains more moisture from the Pacific Ocean, which, combined with the increased cyclonic shear on the jet’s poleward flank, increases the likelihood of precipitation over the southwestern United States. In La Niña years a southward shift in the Pacific storm track is associated with a mean increase in precipitation over the Pacific Northwest. Over the southwestern United States, the weakened subtropical jet decreases the likelihood of precipitation.

Most previous studies have examined ENSO relationships with respect to seasonal mean temperature and precipitation or April 1 snowpack conditions. Not widely examined is how El Niño and La Niña events modulate the seasonal evolution of the montane snowpack. Since many water management decisions are based not on April 1 conditions, but on snowpack conditions 2–3 months prior to peak accumulation, knowledge of differences in ENSO signals through the snow accumulation season can aid in the development of more effective strategies for water management in river systems dependent on snow melt. For example, if high spring runoff is expected, managers may release water from reservoirs in winter to generate additional hydropower. In consideration, the present study focuses attention on the two major river basins in the western United States, the Columbia and the Colorado, and addresses the following questions: (1) What are the mean differences in the

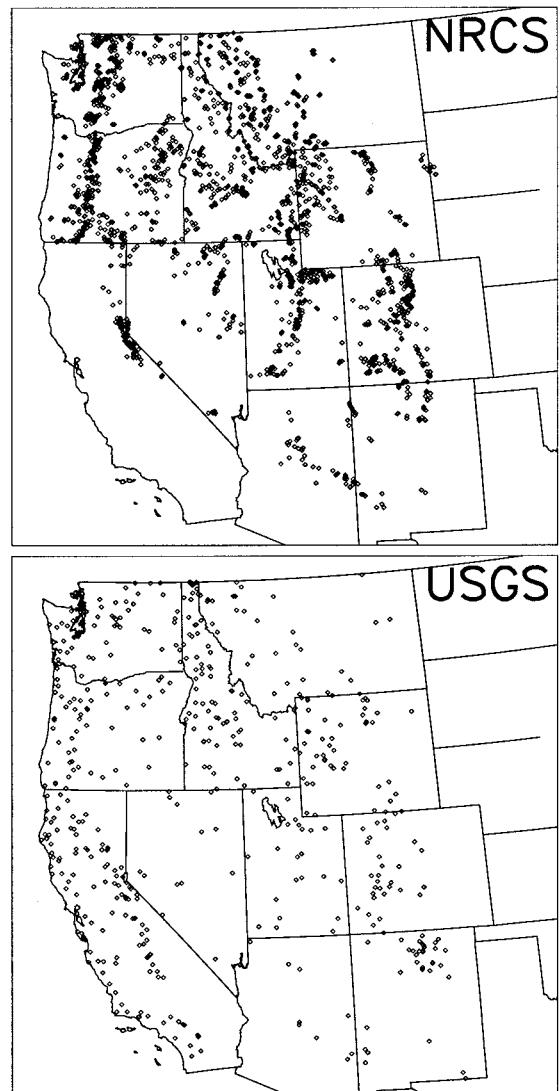


Figure 1. Locations of (top) snow course sites and (bottom) stream gauges in the western United States.

seasonal evolution of the montane snowpack within the Columbia and Colorado River systems during El Niño and La Niña years? (2) To what extent can knowledge of the seasonality in ENSO associations be used to predict runoff?

2. Data

2.1. Snow Course Data

We employ snow-water equivalent (SWE) data collected manually at permanent snow courses maintained by the U.S. Department of Agriculture (USDA) cooperative snow survey program. The program is coordinated by the Natural Resources Conservation Service (NRCS), which has partners conducting measurements in Arizona, Colorado, Idaho, Montana, Nevada, New Mexico, Oregon, South Dakota, Utah, Washington, and Wyoming. The California Department of Water Resources has an independent program. The locations of snow courses included in the USDA archive are illustrated in Figure 1. The number of snow course locations visited started with <10 in the 1910s to almost 2000 in the 1970s (Figure 2). SWE is generally measured on or about the beginning of each month

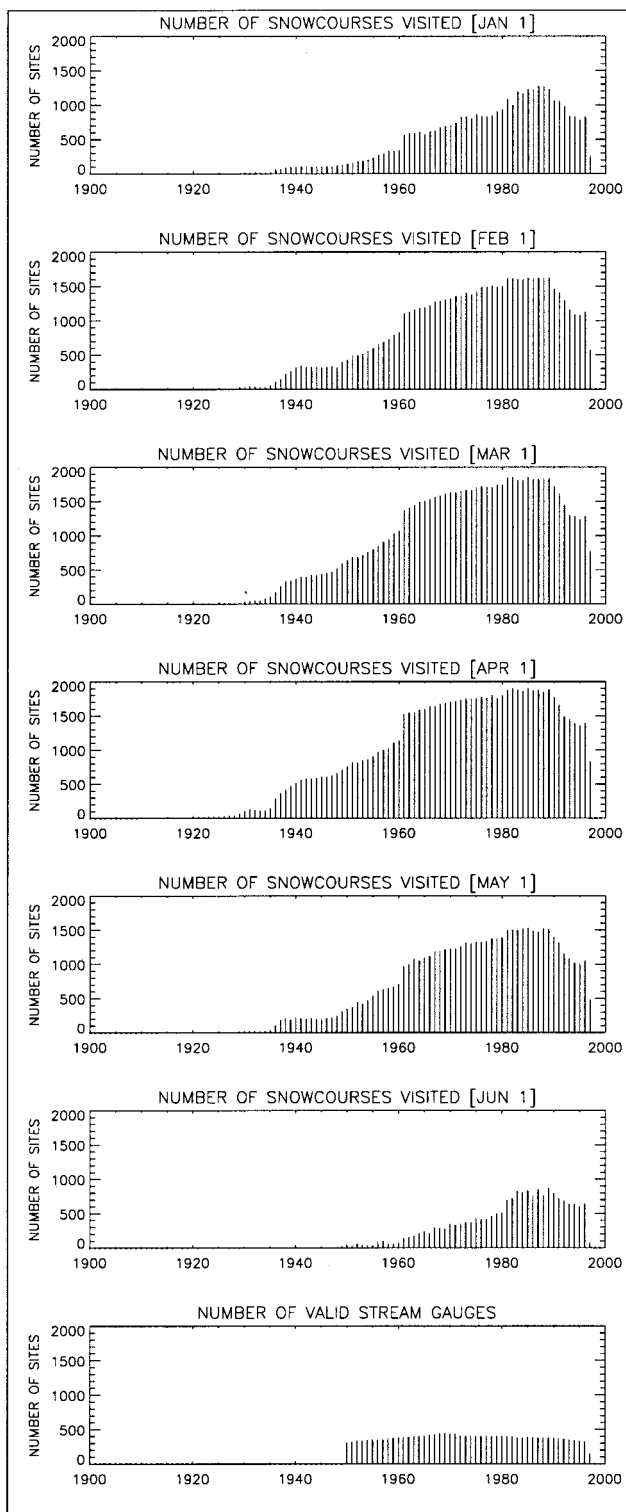


Figure 2. Number of snow course sites visited and number of valid stream gauges in each year. For a stream gauge to be valid, it must have complete daily records for the entire water year. The recent decrease in the number of snow courses visited reflects increasing reliance on the SNOTEL system.

from January through June. Additional measurements may be taken in the middle of the month if knowledge of snowpack conditions is deemed critical. Snow courses are most frequently measured at the beginning of April (Figure 2), repre-

senting the peak SWE in many regions. The frequency and timing of the measurements vary considerably with locality, nature of the snowpack, difficulty of access, and cost [Natural Resources Conservation Service (NRCS), 1988]. (The snow course data were obtained from the USDA NRCS anonymous ftp server wccdmf.wcc.nrcs.usda.gov.)

SWE is measured by pushing a tube down through the snowpack to the ground surface and extracting a core, weighing the tube with its snow core and subtracting the weight of the empty tube. Between 5 and 10 cores are taken at regular intervals along each snow course. The average of all samples is used to represent the snow course value. Generally, the courses are ~1000 feet (305 m) long and are situated in small meadows protected from the wind [NRCS, 1988]. Possible problems with the snow course measurements include changes in vegetation (and hence patterns of snow accumulation) along the snow course, the inability to measure at every snow course site on the first day of every month, and errors in data entry. We undertook no quality control of the snow course data. The effects of any errors in the data set will tend to be reduced through use of basinwide SWE estimates (described in section 2.3).

The snow course data are used because of the long record lengths available. Another source of SWE data is snowpack telemetry (SNOTEL) records, available for over 600 sites in the western United States [Serreze *et al.*, 1999]. SNOTEL sites are automated and unattended and measure SWE using snow “pillows,” which measure the weight of the overlying snowpack. Data are transmitted to a receiving station on a daily basis. SNOTEL was designed to provide cost-effective data from high snow accumulation regions throughout the western United States to supplement and, to some extent, replace monthly snow course records (note in Figure 2 the recent decline in the number of snow course sites visited). While SNOTEL sites have the advantage of daily resolution (and also provide precipitation and temperature measurements), records at most sites extend back only to the early 1980s, largely precluding assessments of variability related to ENSO. We use these data to assess mean seasonal cycles in SWE. Serreze *et al.* [1999] summarize western U.S. SWE conditions using the SNOTEL archive.

2.2. Stream Flow Data

Daily stream flow data from 489 active and discontinued stream gauges throughout the western United States (Figure 1) were extracted from the U.S. Geological Survey on-line database (available at <http://waterdata.usgs.gov/nwis-w/US/>) for water years 1949/1950 to 1996/1997. These gauges were located in basins identified by Slack and Landwehr [1992] as being free of anthropogenic influences, such as flow diversion or augmentation, regulation of the streamflow by containment structures, reduction of base flow by extreme groundwater pumping, or changes in land use (e.g., deforestation) within the basin. Because of extensive regulation of water in the West, there are much fewer valid stream gauges available for analysis than snow course sites (Figure 2). However, as described in section 2.3, measurements of streamflow integrate heterogeneities in surface climate across a drainage basin.

2.3. Computation of Basin-Wide SWE and Runoff Estimates

To focus attention on regional-scale associations, basinwide estimates of SWE and runoff are computed for major subba-

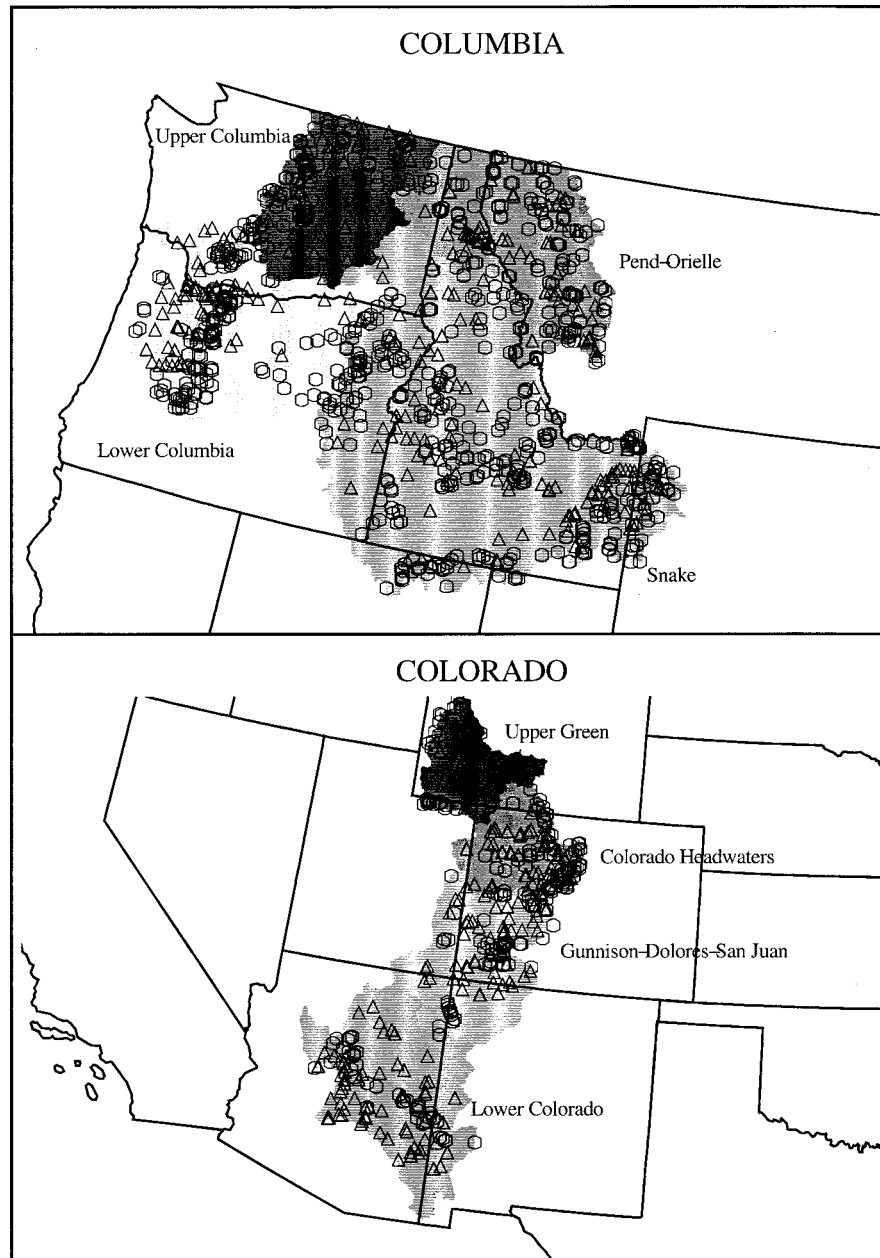


Figure 3. Snow course sites (circles) and stream gauges (triangles) in subbasins within the Columbia and Colorado River Basins. See Table 2 for additional information.

sins in the Columbia and Colorado watersheds. Snow courses and stream gauges were classified into drainage basins based on the Hydrologic Unit Code [Seaber *et al.*, 1987]. For the Columbia River the subbasins selected within the United States are the (1) Upper Columbia and Yakima, (2) Pend Orielle and Kootenai, (3) Snake River, and (4) Lower Columbia (Figure 3). The subbasins selected in the Colorado River Basin include the (1) Upper Green, (2) Colorado Headwaters, the White River, and the Yampa, (3) San Juan, Gunnison, and Dolores, and (4) Lower Colorado (Figure 3). Further descriptions of these basins and the number of snow courses and stream gauges available within them are provided in Tables 1 and 2.

While there are a large number of snow course sites and stream gauges available in each basin, there are few with com-

plete records (Table 2). Estimating regional-mean SWE and annual runoff by simply averaging all sites available in each year may result in biases especially if the mean elevation (or aspect) of the snow course sites that are visited in a basin varies markedly over time. To correct for such biases, the time series for each snow course were converted into a series of z scores (by subtracting the long-term snow course mean and dividing by the snow course standard deviation). For each year the z scores were then averaged for all snow courses reporting in the basin. We then averaged the long-term mean and standard deviation for all snow courses in the basin, and used these values to convert the basinwide z score time series back to units of water equivalent (mm). To be included in the basinwide averages, a snow course must have been visited on at least 50% of the years between 1951 and 1996. For a given year and

Table 1. Description of the Selected Subbasins^a

Basin	Description
Columbia River Basin	
Upper Columbia and Yakima	
Subregion 1702	Columbia River Basin within the United States above the confluence with the Snake River Basin, excluding the Yakima River Basin
Subregion 1703	Yamima River Basin
Pend Orielle and Kootenai	
Subregion 1701	Kootenai, Pend Orielle, and Spokane River Basins within the United States
Snake	
Subregion 1704, Upper Snake	Snake River Basin to and including the Clover Creek Basin
Subregion 1705, Middle Snake	Snake River Basin below the Clover Creek Basin to Hells Canyon Dam
Subregion 1706, Lower Snake	Snake River Basin below Hells Canyon Dam to its confluence with the Columbia
Lower Columbia	
Subregion 1707, Middle Columbia	Columbia River Basin below the confluence with the Snake River Basin to Bonneville Dam
Subregion 1708, Lower Columbia	Columbia River Basin below Bonneville Dam, excluding the Willamette Basin
Subregion 1709, Willamette	Willamette River Basin, Oregon
Colorado River Basin	
Upper Green	
Subregion 1404, Great Divide-Upper Green	Green River Basin above the confluence with the Yampa River Basin and the Great Divide closed basin
Colorado headwaters and the White and Yampa	
Subregion 1401, Colorado Headwaters	Colorado River Basin to but excluding the Bitter Creek Basin and excluding the Gunnison River Basin
Subregion 1405	White and Yampa River Basins
Gunnison/Dolores/San Juan	
Subregion 1402, Gunnison	Gunnison River Basin
Subregion 1403, Upper Colorado-Dolores	Colorado River Basin from and including the Bitter Creek Basin to the confluence with the Green River Basin
Subregion 1408, San Juan	San Juan River Basin
Lower Colorado	
Subregion 1502	Little Colorado River Basin
Subregion 1504, Upper Gila	Gila River Basin above Coolidge Dam, including the Animas Valley closed basin
Subregion 1506	Salt River Basin

^aFrom *Seaber et al.* [1987].

month, basinwide means were only taken as valid if at least five snow courses were reporting. Identical procedures were employed to compute basinwide estimates of runoff.

Because of strong topographic controls, SWE varies markedly at different sites throughout each subbasin [Serreze *et al.*, 1999]. Generating estimates of SWE and runoff over large river basins may mask (or “smooth”) heterogeneities in ENSO associations. To assess the degree of spatial coherence in SWE and runoff in each river basin, we computed the correlation between interannual variations in the basinwide estimates and interannual variations at each individual snow course site and stream gauge in the basin. The distribution of correlations for each subbasin is presented in Figure 4 as box and whisker plots for April 1 SWE (Figure 4, left) and annual runoff (Figure 4, right). The median correlation for April 1 SWE is generally between 0.8 and 0.9, illustrating that the basinwide mean is representative of variability in conditions throughout the basin. Results for other months exhibit similar patterns (not shown). The rare low correlations imply that there are always a few snow course sites that have very site-specific responses to regional climate forcing. For annual runoff the spatial coherence is stronger than for April 1 SWE. Median correlations are generally above 0.9, and minimum correlations are generally above 0.5. Correlations for the large Snake River Basin are naturally slightly lower. The stronger spatial coherence for annual runoff is not surprising, as spatial heterogeneities in SWE are integrated across the watershed.

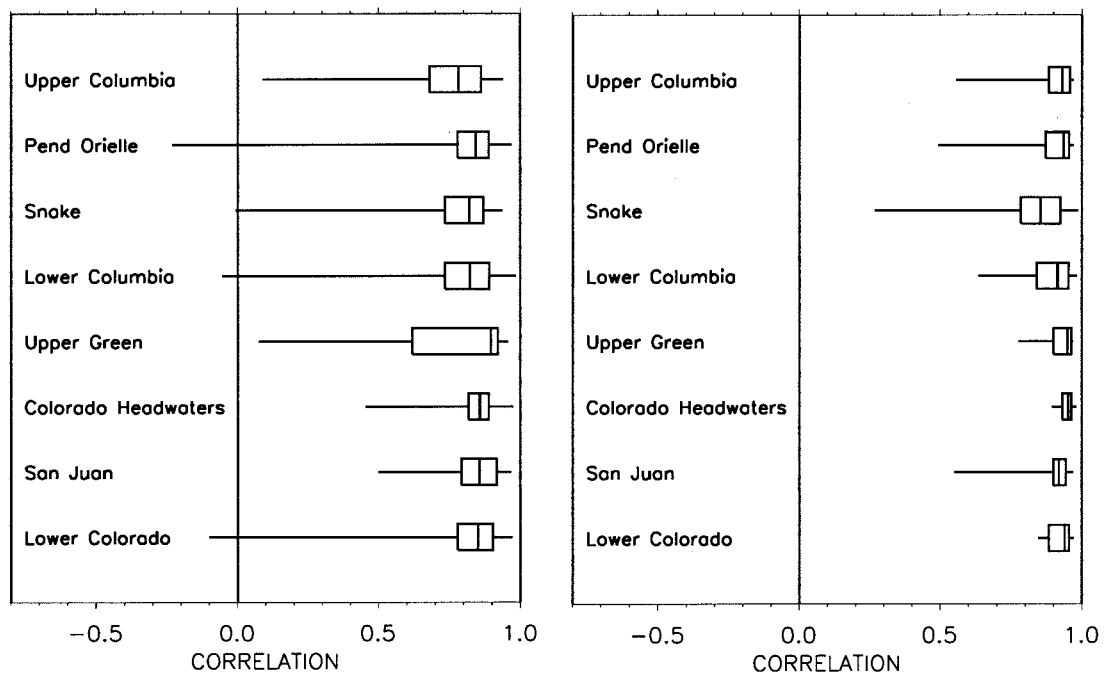
3. General Climatic Features

It is useful to start with a brief discussion of the climatological characteristics of SWE and runoff for the major subbasins. Analyses focus on (1) mean seasonal cycles of SWE and runoff in each subbasin and (2) the utility of SWE in predicting runoff.

Figures 5 and 6 show respectively the mean seasonal cycles in SWE and runoff for the subbasins examined in the Columbia and Colorado River systems. To provide daily resolution of SWE, the seasonal cycles in SWE are based on SNOTEL data. To be used, the SNOTEL records for each site had to be at least 5 years in length. In the Columbia River Basin (Figure 5) the basinwide mean hydrographs in all subbasins, apart from the Lower Columbia, are dominated by spring snow melt. In this region, between 50% and 60% of the annual precipitation in these regions falls as snow [Serreze *et al.*, 1999], and in summer, much of the precipitation is offset by evaporative losses [Kohler *et al.*, 1959]. However, in the lower elevation coastal Lower Columbia River Basin, a spring runoff maximum in the mean annual hydrograph is not observed. Here, more precipitation falls as rain, and the largest runoff occurs in autumn and winter when precipitation totals are highest [see Serreze *et al.*, 1999]. In the Colorado River system the basinwide mean hydrographs also exhibit a spring maximum in runoff in most basins (Figure 6), illustrating the strong role of snow in the surface water resources in this region. In compar-

Table 2. Number of Snow Course Sites and Stream Gauges (in Undisturbed Drainages) Reporting in Each Subbasin Over the Period 1951–1996

	Completeness of Records, %	Jan. 1 SWE	Feb. 1 SWE	March 1 SWE	April 1 SWE	May 1 SWE	June 1 SWE	Water Year Runoff
Columbia River								
Upper Columbia/Yakima	25	35	60	62	63	48	21	17
	50	15	37	39	39	28	2	16
	75	9	25	28	29	10	0	12
	100	0	4	3	8	0	0	5
Pend-Orielle	25	94	105	164	165	152	76	30
	50	62	68	137	145	124	37	27
	75	45	49	95	128	80	8	19
	100	8	12	28	41	22	3	13
Snake	25	250	317	348	354	258	116	65
	50	185	260	303	313	188	43	44
	75	129	186	225	237	120	27	26
	100	20	36	53	72	11	2	18
Lower Columbia	25	111	135	138	137	117	64	30
	50	46	63	66	68	43	7	27
	75	17	28	29	30	17	0	23
	100	0	8	4	9	1	0	12
Colorado River								
Upper Green	25	17	32	35	38	33	16	10
	50	0	25	32	37	31	3	5
	75	0	19	24	27	21	0	5
	100	0	0	5	5	0	0	0
Colorado Headwaters	25	27	72	72	75	75	24	9
	50	10	59	59	60	60	9	9
	75	4	50	52	52	52	6	7
	100	0	20	24	29	23	1	4
Gunnison/Dolores/San Juan	25	31	55	55	54	50	26	19
	50	15	37	43	44	44	12	17
	75	4	28	37	37	36	5	13
	100	0	9	9	12	10	0	10
Lower Colorado	25	45	53	51	53	18	16	11
	50	11	34	38	37	0	0	11
	75	0	20	20	18	0	0	8
	100	0	4	10	2	0	0	7

**Figure 4.** Distribution of Pearson correlation coefficients in each basin (left) between the basin mean time series of April 1 SWE and the April 1 SWE time series at each individual snow course site and (right) between the basin mean time series of annual runoff and the annual runoff time series at each individual stream gauge.

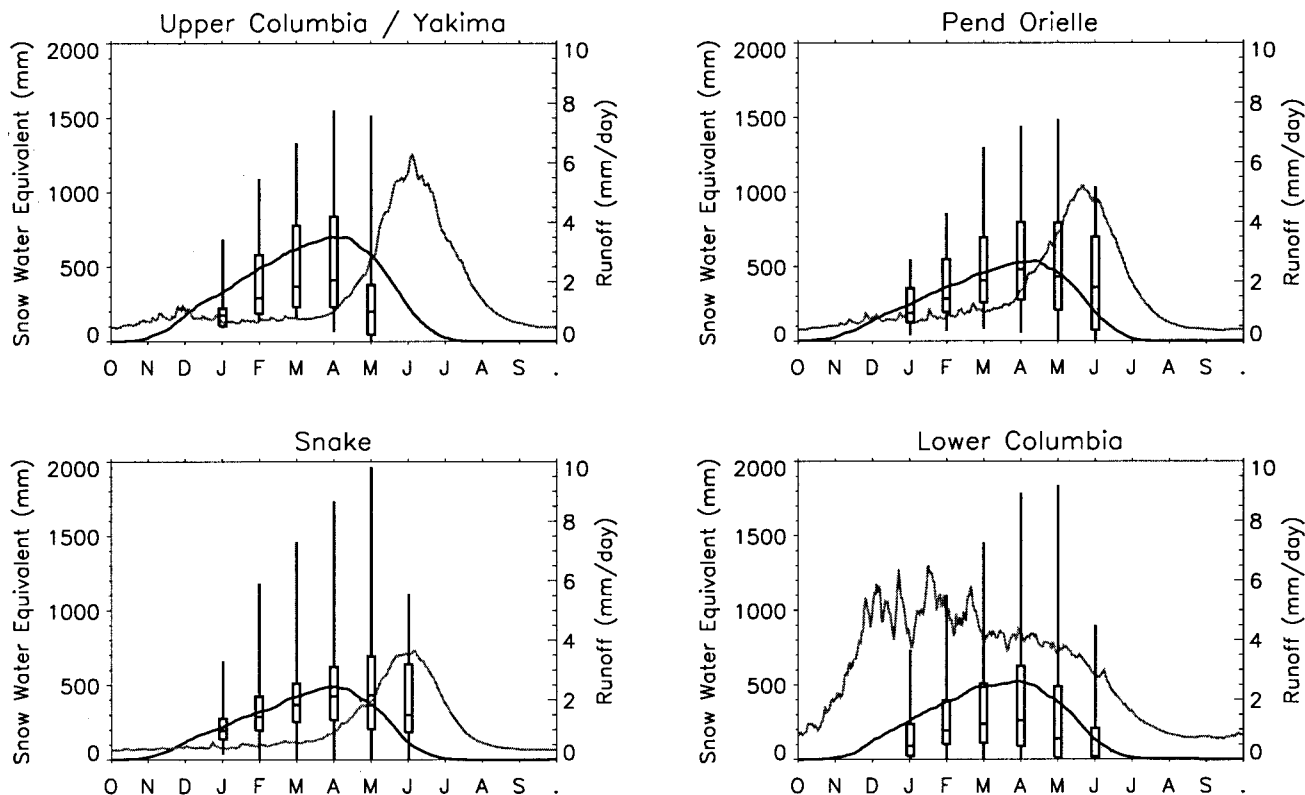


Figure 5. Mean seasonal cycles of SWE and runoff for subbasins in the Columbia River system. The dark solid line shows the mean basinwide seasonal cycle in SWE from SNOTEL sites (daily resolution), the solid shaded line shows the basinwide mean seasonal cycle in runoff, and the box and whiskers outlines illustrate the minimum, lower quartile, median, upper quartile, and maximum mean SWE for each individual snow course site in the basin.

ison to the subbasins of the Columbia River system, runoff totals in this moisture limited region are smaller. Note the extremely low SWE and runoff totals and the absence of a spring runoff peak in the warm Lower Colorado River Basin.

The strong influence of snow on surface water resources for most basins illustrates that the amount of water stored in the snowpack at its seasonal peak (e.g., April 1) can provide a good predictor of the amount of runoff over the remainder of the water year. Indeed, such relationships formed the rationale for development of the snow course network in the 1930s. To quantify the benefits of measuring the water stored in the seasonal snowpack, correlations were computed between January 1 SWE, February 1 SWE, March 1 SWE, April 1 SWE, and May 1 SWE and runoff for the remainder of the water year (e.g., for January 1 SWE, runoff for the remainder of the water year would be for the period January 1 through September 30). Correlations are only computed if there are at least 20 overlapping years of valid data in the basinwide SWE and runoff time series. Results from this experiment are summarized in Table 3. Correlations are moderately strong (mostly above 0.5) in midwinter (e.g., January 1). At the peak of the accumulation season (approximated by April 1), correlations are much higher (generally above 0.8 and, in some cases, above 0.9), illustrating the remarkable degree of predictive skill that can be realized from knowledge of amount of water stored in the seasonal snowpack. Correlations are weaker in the Lower Columbia and Lower Colorado River Basins, where more of the annual precipitation falls as rain. While ENSO predictions can be realized in autumn before any snow has accumulated, many

water management decisions (e.g., reservoir releases) are made in the middle of winter when some predictive skill can be extracted from the snowpack itself. The challenge is to identify ways in which one can improve upon predictions based on persistence. This issue is addressed in sections 4 and 5.

4. Composite ENSO SWE and Runoff Associations

4.1. Construction of the Composites

To identify general relationships between ENSO and SWE, it is instructive to first construct composites of mean anomalous SWE in El Niño and La Niña years. The first step in this analysis is to identify “El Niño” and “La Niña” years. Any such classification is somewhat arbitrary. Our definition is based on mean November through April (corresponding to the accumulation season in most of the western United States) values of the Niño 3.4 index. The Niño 3.4 index represents the average SST anomaly in the central equatorial Pacific Ocean (5°N – 5°S ; 170°W – 120°W), where tropical convection is most sensitive to SST variations [Trenberth, 1997; Hoerling et al., 1997]. We simply ranked each year over the period 1951–1996 in terms of the mean wintertime anomaly value (Table 4), and designated the 10 warmest (coldest) years as El Niño (La Niña) events. Attention is restricted to years after 1951, as the earlier SST data are somewhat unreliable. Using average values of these ENSO indices for November through April places implicit reliance on the ability to predict the ENSO state several months in ad-

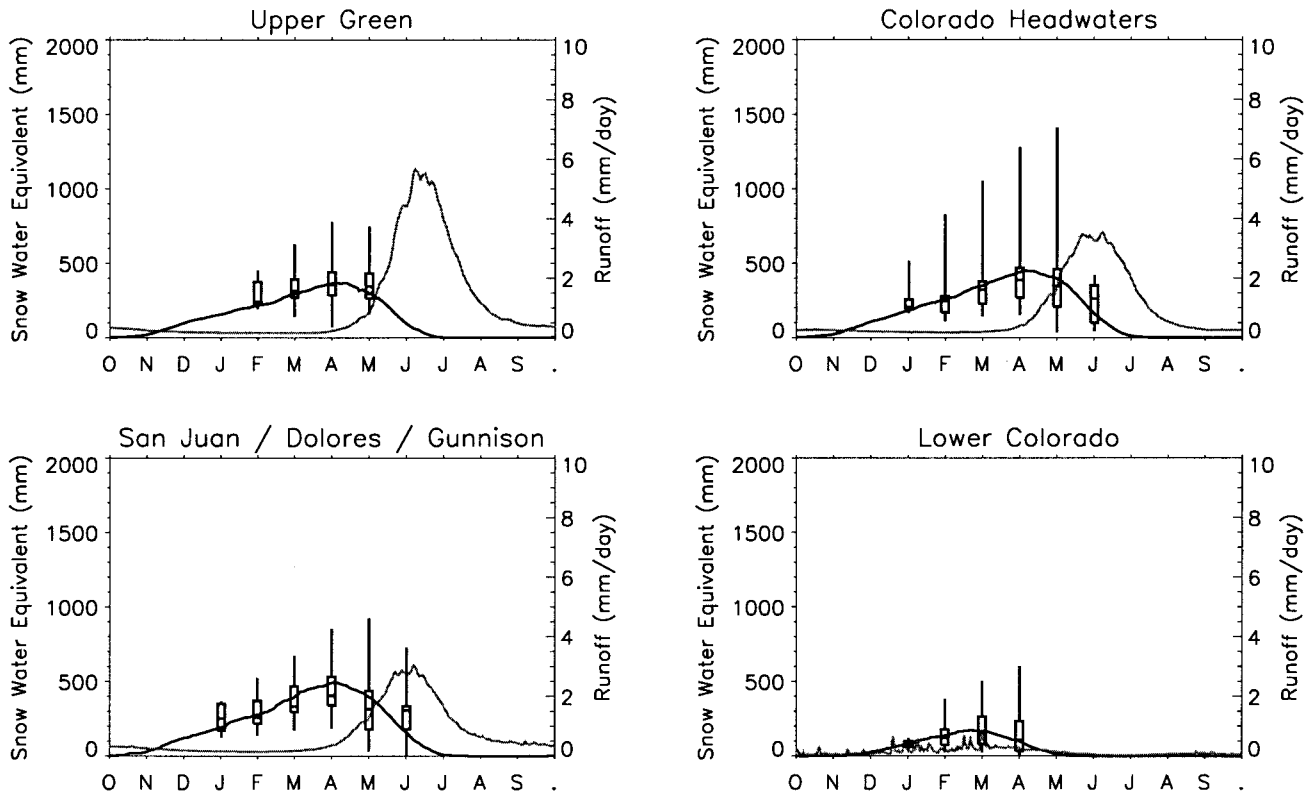


Figure 6. Mean seasonal cycles of SWE and runoff for subbasins in the Colorado River system. The dark solid line shows the mean basinwide seasonal cycle in SWE from SNOTEL sites (daily resolution), the solid shaded line shows the basinwide mean seasonal cycle in runoff, and the box and whiskers outlines illustrate the minimum, lower quartile, median, upper quartile, and maximum mean SWE for each individual snow course site in the basin.

vance. Long-lead predictions of the presence/absence of El Niño and La Niña events are feasible [Penland and Magorian, 1993; Ji *et al.*, 1994, 1998; Chen *et al.*, 1997] and represent an improvement upon persistence (e.g., if we used instead a prewinter value of the Niño 3.4 index or the SOI).

To construct the composites, the anomalous SWE for each basin was averaged on a seasonal basis for the 10 strongest El Niño and 10 strongest La Niña years as defined by the Niño 3.4 index. Differences between individual El Niño and La Niña events also were examined by plotting the anomalous SWE for each of the 10 years that make up the two composites. To address potential problems arising from the small sample size, sensitivity tests were conducted by substituting the Niño 3.4 index with the Southern Oscillation index (Table 4) and by

varying the number of El Niño or La Niña years in the composites. Significance testing is achieved through the use of *t* tests [Panofsky and Brier, 1968].

4.2. Columbia River Basin

Composite anomalies and inter-ENSO variability in SWE and annual runoff for the subbasins in the Columbia River are illustrated in Figure 7. Consistent with previous work [e.g., Cayan and Webb, 1992], there is a general tendency for decreased SWE and annual runoff during El Niño years and increased SWE and annual runoff in La Niña years. In the broadest sense, these associations reflect decreases (increases) in precipitation and increases (decreases) in temperature associated with a northward (southward) displacement of the

Table 3. Correlations Between SWE at Various Points in the Accumulation Season and Runoff for the Remainder of the Water Year

	Jan. 1 SWE	Feb. 1 SWE	March 1 SWE	April 1 SWE	May 1 SWE
Upper Columbia/Yakima	0.56	0.72	0.77	0.83	0.83
Pend-Orielle	0.48	0.71	0.82	0.86	0.88
Snake	0.75	0.82	0.86	0.90	0.91
Lower Columbia	0.51	0.51	0.64	0.60	0.61
Upper Green	No data	0.80	0.86	0.87	0.93
Colorado Headwaters	0.70	0.74	0.73	0.81	0.89
Gunnison/Dolores/San Juan	0.60	0.71	0.73	0.84	0.90
Lower Colorado	0.52	0.68	0.67	0.76	No data

Table 4. Years Ranked in Terms of the Magnitude of the Nino 3.4 Index and the Southern Oscillation Index^a

	Rank	Nino 3.4	SOI
La Nina	1	1989	1974
	2	1974	1971
	3	1971	1989
	4	1976	1976
	5	1956	1956
	6	1985	1951
	7	1955	1967
	8	1996	1962
	9	1951	1963
	10	1984	1960
	11	1975	1955
	12	1968	1975
	13	1965	1982
	14	1986	1985
	15	1967	1972
	16	1972	1996
	17	1963	1957
	18	1962	1984
	19	1981	1961
	20	1961	1968
	21	1957	1986
	22	1960	1954
	23	1990	1979
	24	1982	1977
	25	1979	1965
	26	1994	1964
	27	1954	1988
	28	1953	1991
	29	1991	1970
	30	1993	1980
	31	1959	1953
	32	1978	1959
	33	1980	1981
	34	1952	1994
	35	1964	1969
	36	1977	1995
El Nino	37	1988	1973
	38	1970	1952
	39	1995	1990
	40	1969	1958
	41	1966	1966
	42	1987	1993
	43	1973	1978
	44	1958	1987
	45	1992	1992
	46	1983	1983

^aThe Nino 3.4 index is the area-averaged SST over the region 170°W–120°N, 5°S–5°N, and the SOI is the sea level pressure difference between Tahiti and Darwin. The SOI is multiplied by -1 to be consistent with the Nino 3.4 index. Years are defined as the date at the end of winter (i.e., the winter of 1982/1983 is taken as 1983).

storm track in El Nino (La Nina) years. However, some seasonality is evident in these results. In El Nino years the snowpack is very close to normal at the beginning of January, and decreases in SWE are only barely apparent by the end of the accumulation season (Figure 7). The only associations significant above the 90% confidence level are for annual runoff in the Upper Columbia/Yakima and for April 1 SWE and annual runoff in the Pend-Orielle River Basin. *Livezey et al.* [1997] illustrate that although precipitation in the Pacific Northwest in El Nino conditions is below normal in October, November, February, and March, it is actually above normal in December and January. These increases in precipitation occur in conjunc-

tion with a midwinter eastward shift of the tropospheric wave train [*Hoerling and Kumar*, 2000]. Since most snow in the Pacific Northwest mountains falls in midwinter [*Serreze et al.*, 1999], the increases in precipitation in December and January offset the effects of decreased precipitation in other months.

In comparison to the weak SWE associations in El Nino years the increases in SWE and annual runoff in La Nina years are relatively strong, with many of the associations significant above the 90% confidence level. In La Nina years a southward shift in the Pacific storm track is associated with mean increases in precipitation over the Pacific Northwest [e.g., *Redmond and Koch*, 1991]. In addition to these mean precipitation increases, *Cayan et al.* [1999] show the frequency of extreme (top 10%) precipitation events to be higher over the Pacific Northwest in La Nina years. These increases are particularly pronounced over the Oregon coast and thus help to explain the large increases in SWE in the Lower Columbia River Basin. *Livezey et al.* [1997] show mean increases in precipitation to occur throughout the accumulation season, particularly marked in November, December, January, and March. These relatively constant increases in precipitation in La Nina years, compared to El Nino years when the general tendency for decreased precipitation is offset by small increases in precipitation in midwinter, explain the lack of symmetry between the opposing ENSO states.

In both the El Nino and La Nina composites, large differences in SWE totals are evident between the individual composite members (Figure 7). With our small sample size the SWE anomaly in a single El Nino or La Nina year can have a large impact on the composite mean. It is hence possible that if the El Nino and La Nina years are defined in a slightly different way, conclusions may change regarding mean associations. To address this issue, sensitivity tests were conducted by varying the number of years in the composites (e.g., using the six strongest El Nino years instead of the 10 strongest) and by replacing the Nino 3.4 index with the SOI (Table 5). Results were found to be insensitive to the years included or the index used. In most of the combinations examined, there is a progression from near normal SWE in midwinter to slightly below normal SWE in April and May in the El Nino composites and large increases in SWE throughout the winter season in the La Nina composites. The only notable difference is a tendency for stronger decreases in SWE in the El Nino composites in April and May, when the Nino 3.4 index is replaced with the SOI.

4.3. Colorado River Basin

Results for Colorado River Basin are presented in an identical manner to those for the Columbia Basin, with mean changes in SWE and annual runoff summarized in Figure 8, and the sensitivity tests documented in Table 6. In El Nino years, mean changes in the seasonal snowpack (Figure 8) depict a transition between drier-than-average conditions in the north (best expressed in the Upper Green) and wetter-than-average conditions in the southwest (best expressed in the Lower Colorado). Broadly opposing patterns are found for La Nina years, supporting results from previous work [e.g., *Cayan and Webb*, 1992]. The associations in the Upper Green are consistent with results for the Columbia River Basin, where the decreases (increases) in SWE in El Nino (La Nina) years reflect the northward (southward) displacement of the storm track and associated decreases (increases) in precipitation. Results from the sensitivity tests conducted for the Upper Green reveal that the associations are relatively insensitive to the

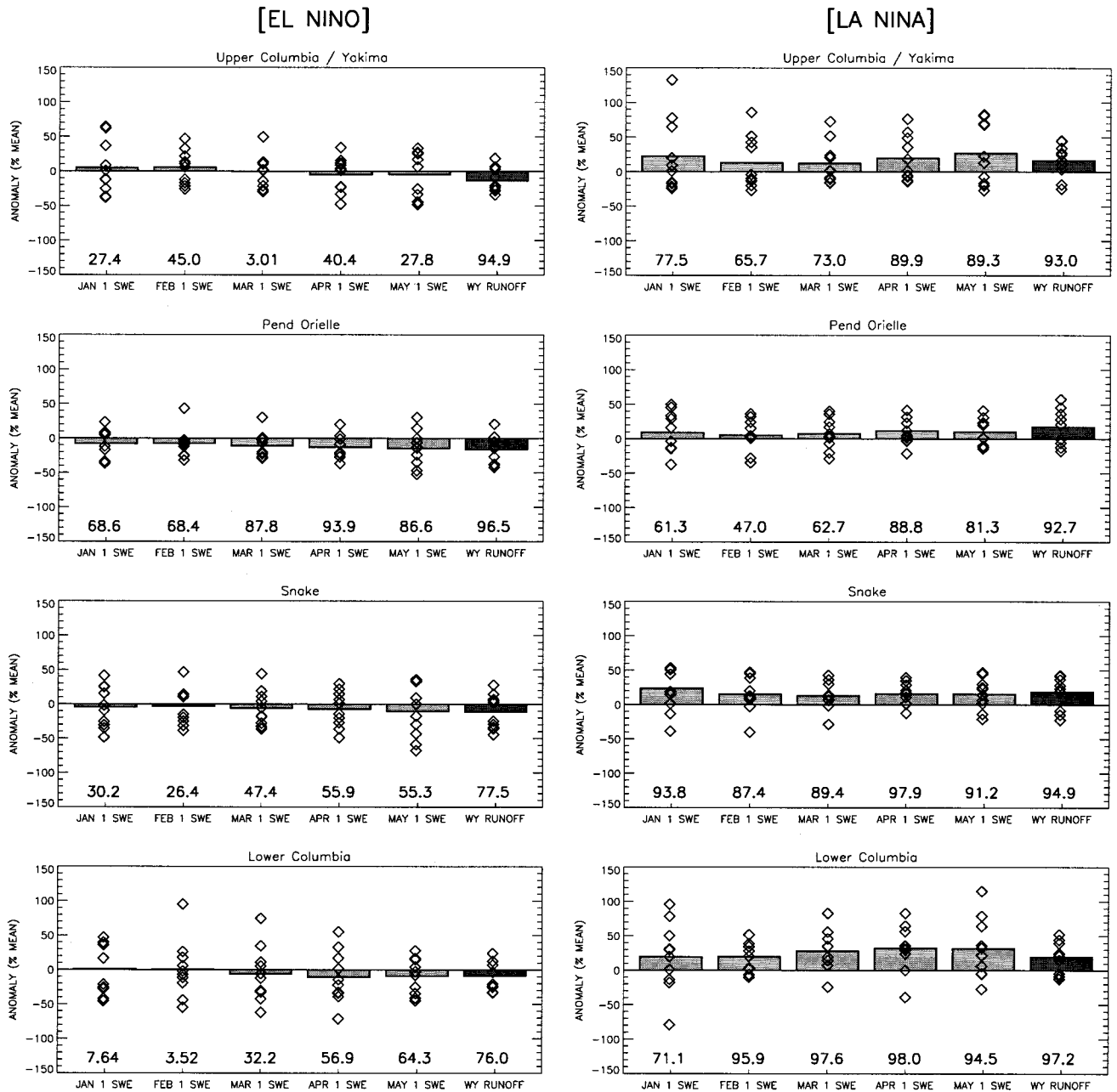


Figure 7. Anomalous monthly SWE and annual runoff (expressed as a percentage of the mean) in El Niño and La Niña years for the major subbasins in the Columbia River basin. The bars represent the composite mean of the 10 strongest El Niño and La Niña years (based on the Niño 3.4 index, Table 4), and the diamonds represent the individual composite members. Significance estimates (in percent) based on t tests are displayed on the bottom of each plot.

number of El Niño and La Niña years included in the composites and the type of index used (Table 6). In the Lower Colorado Basin the significant increases (decreases) in SWE in El Niño (La Niña) years occur in part due to the changes in precipitation associated with a strengthening (weakening) of the subtropical jet.

An interesting feature of Figure 8 is that the SWE anomalies in the Lower Colorado Basin increase in magnitude over the winter season, and tend to be much more pronounced on April 1 than on March 1. Since the mean date of maximum SWE in this region is typically around February 20 [Serreze *et al.*, 1999], these associations reflect a prolonged accumulation season in

El Niño years and earlier melt in La Niña years. There is some evidence of similar seasonal changes in the Colorado Headwaters and the Gunnison, Dolores, and San Juan River Basins, but these are much more subdued (Figure 8). Sensitivity tests show that while the seasonal changes in SWE are fairly robust in the Lower Colorado River Basin, the associations in the Colorado Headwaters and the San Juan River Basin are sensitive to both the number of years included in the composites and the type of index used (Table 6). Note in particular that the large midwinter increases in SWE in the Colorado Headwaters in La Niña years (Figure 8) are nonexistent when the Niño 3.4 index is replaced with the SOI.

Table 5. Mean Anomalous SWE and Annual Runoff for the Columbia River Basin^a

	Variable	Nino 3.4 Years in Composite					SOI Years in Composite				
		6	8	10	12	14	6	8	10	12	14
<i>El Nino</i>											
Upper Columbia	Jan. 1 SWE	-11.23	7.39	4.84	-3.02	-5.35	4.21	-4.08	-7.66	6.07	0.60
	Feb. 1 SWE	-4.33	6.72	5.54	-1.15	0.73	1.17	-0.22	0.61	7.22	0.12
	March 1 SWE	-9.07	0.93	-0.33	-6.19	-3.80	-3.49	-3.20	-2.93	2.78	-1.41
	April 1 SWE	-13.38	-3.79	-4.95	-7.29	-5.45	-11.72	-10.14	-10.31	-4.44	-9.38
	May 1 SWE	-12.91	-5.82	-4.54	-8.27	-11.58	-18.50	-13.68	-19.54	-13.97	-18.91
	Annual runoff	-15.99	-10.74	-13.65	-14.79	-13.36	-12.20	-10.06	-11.80	-9.07	-10.04
Pend-Orielle	Jan. 1 SWE	-7.15	-1.39	-8.16	-12.08	-8.56	2.38	-0.63	4.26	6.42	1.82
	Feb. 1 SWE	-12.69	-5.10	-7.80	-9.93	-7.53	-5.94	-5.68	-3.54	0.07	-5.27
	March 1 SWE	-14.78	-10.14	-11.01	-13.03	-10.86	-11.09	-8.28	-6.59	-4.84	-8.56
	April 1 SWE	-18.14	-13.91	-12.85	-12.01	-9.67	-19.58	-15.41	-12.84	-10.91	-14.24
	May 1 SWE	-21.50	-17.80	-14.68	-14.36	-15.83	-24.14	-19.68	-19.82	-17.69	-20.54
	Annual runoff	-21.85	-14.45	-16.63	-18.26	-16.54	-16.73	-12.72	-13.55	-10.00	-10.64
Snake	Jan. 1 SWE	-5.60	2.10	-4.39	-12.09	-7.29	2.96	-2.20	4.78	8.47	2.55
	Feb. 1 SWE	-13.83	-2.79	-3.31	-8.82	-3.65	-6.21	-6.67	-1.11	4.16	-2.42
	March 1 SWE	-12.43	-4.45	-5.92	-11.65	-6.72	-5.37	-5.41	-1.17	2.34	-2.64
	April 1 SWE	-13.77	-6.46	-7.22	-9.85	-4.71	-14.50	-12.76	-6.78	-3.03	-8.01
	May 1 SWE	-17.17	-11.73	-10.42	-13.06	-11.34	-17.56	-15.35	-12.36	-9.61	-15.34
	Annual runoff	-17.01	-10.10	-11.17	-13.42	-10.25	-12.29	-12.03	-10.16	-6.70	-9.66
Lower Columbia	Jan. 1 SWE	-4.02	7.80	1.35	-6.66	-2.60	10.42	0.33	4.97	11.95	2.61
	Feb. 1 SWE	-10.65	4.65	0.66	-3.84	0.15	-0.89	-3.61	1.00	9.46	0.83
	March 1 SWE	-9.82	-2.08	-5.92	-9.20	-5.07	1.73	1.21	4.51	7.47	-0.31
	April 1 SWE	-13.53	-7.35	-10.73	-8.32	-3.45	-15.34	-12.46	-6.38	-3.18	-10.10
	May 1 SWE	-16.06	-10.51	-9.30	-7.85	-8.46	-18.70	-15.25	-15.57	-12.01	-15.68
	Annual runoff	-13.38	-7.60	-8.95	-12.14	-11.08	-8.21	-7.38	-8.66	-5.51	-8.12
<i>La Nina</i>											
Upper Columbia	Jan. 1 SWE	43.79	27.18	22.73	18.06	18.95	46.01	28.74	12.59	10.30	11.55
	Feb. 1 SWE	24.30	13.26	12.80	11.53	11.56	32.15	23.74	9.15	7.05	6.59
	March 1 SWE	20.51	13.54	12.02	11.17	10.42	26.11	17.71	5.50	5.68	5.04
	April 1 SWE	31.43	22.16	19.85	17.51	14.08	38.42	29.43	15.30	15.84	13.69
	May 1 SWE	34.56	32.53	26.60	25.50	18.79	39.07	38.67	25.31	32.31	28.38
	Annual runoff	14.64	15.70	16.31	14.10	11.20	22.80	17.30	13.32	11.40	9.02
Pend-Orielle	Jan. 1 SWE	26.75	14.92	9.12	7.38	7.29	18.19	12.54	6.89	2.21	5.02
	Feb. 1 SWE	18.33	9.96	5.31	5.57	5.66	18.71	19.79	12.35	8.67	8.73
	March 1 SWE	19.07	11.90	7.34	7.13	7.53	19.91	21.29	13.52	11.21	11.00
	April 1 SWE	22.35	16.04	11.89	11.00	9.66	23.99	25.06	16.16	15.18	14.67
	May 1 SWE	15.54	14.28	10.14	12.65	10.63	17.06	24.18	17.78	20.78	19.68
	Annual runoff	17.51	18.06	17.23	13.79	12.86	25.21	20.29	16.59	13.70	11.70
Snake	Jan. 1 SWE	38.93	22.71	23.66	16.72	19.81	33.57	24.40	8.88	3.07	8.55
	Feb. 1 SWE	26.19	15.91	15.23	10.84	13.21	28.86	25.58	11.63	6.14	7.57
	March 1 SWE	20.98	12.93	13.03	10.47	13.55	23.93	20.07	9.35	6.62	7.43
	April 1 SWE	22.78	15.68	15.85	13.72	14.24	25.45	20.93	10.36	9.95	11.09
	May 1 SWE	16.04	15.69	15.69	17.44	17.12	19.36	23.71	15.25	20.45	19.41
	Annual runoff	18.68	15.81	18.82	15.79	18.40	23.31	16.62	11.22	8.99	9.47
Lower Columbia	Jan. 1 SWE	43.41	22.78	19.49	14.96	20.01	27.51	16.48	2.19	2.26	13.78
	Feb. 1 SWE	31.57	21.64	19.67	14.64	15.89	31.32	22.98	8.30	6.75	12.81
	March 1 SWE	44.70	31.42	27.76	20.93	20.59	43.41	31.47	16.39	16.32	18.37
	April 1 SWE	48.74	36.16	32.03	25.69	20.90	51.12	39.11	23.37	26.55	26.73
	May 1 SWE	39.78	40.79	31.63	28.23	20.92	37.52	38.40	26.44	37.07	35.41
	Annual runoff	19.80	18.19	19.33	15.01	14.00	25.86	16.90	12.37	9.79	9.62

^aComputed using the (x) strongest El Nino years and the (x) strongest La Nina years (Table 4) for the Nino 3.4 index and the SOI. Composites are tabulated if at least 70% of the years hold valid data. Values are given as percent of the mean.

5. Cross-Validated Prediction Experiments

The results just presented suggest that ENSO information may be used to enhance hydrologic predictions in many sub-basins in the Columbia and Colorado River systems. In some river basins the ENSO associations are weak and, by themselves, will provide little benefit for seasonal runoff forecasts. However, our analysis shows that in some instances the change in the ENSO association throughout the accumulation season is often greater than the mean ENSO association in any given month. For example, in the Upper Columbia/Yakima River Basin, the small midwinter increases in SWE in El Nino years

shift to small decreases in SWE at the end of the accumulation season and significant decreases in annual runoff. It is possible that combining information on the water equivalent of the snowpack at any point in the accumulation season with knowledge of seasonal changes in the ENSO association may improve seasonal water supply outlooks.

To test these ideas, we attempt to predict runoff in each of the subbasins examined. Three predictive schemes are examined: ENSO, persistence, and persistence and ENSO.

1. In the ENSO scheme, runoff anomalies in a given El Nino or La Nina year are simply equal to the mean runoff

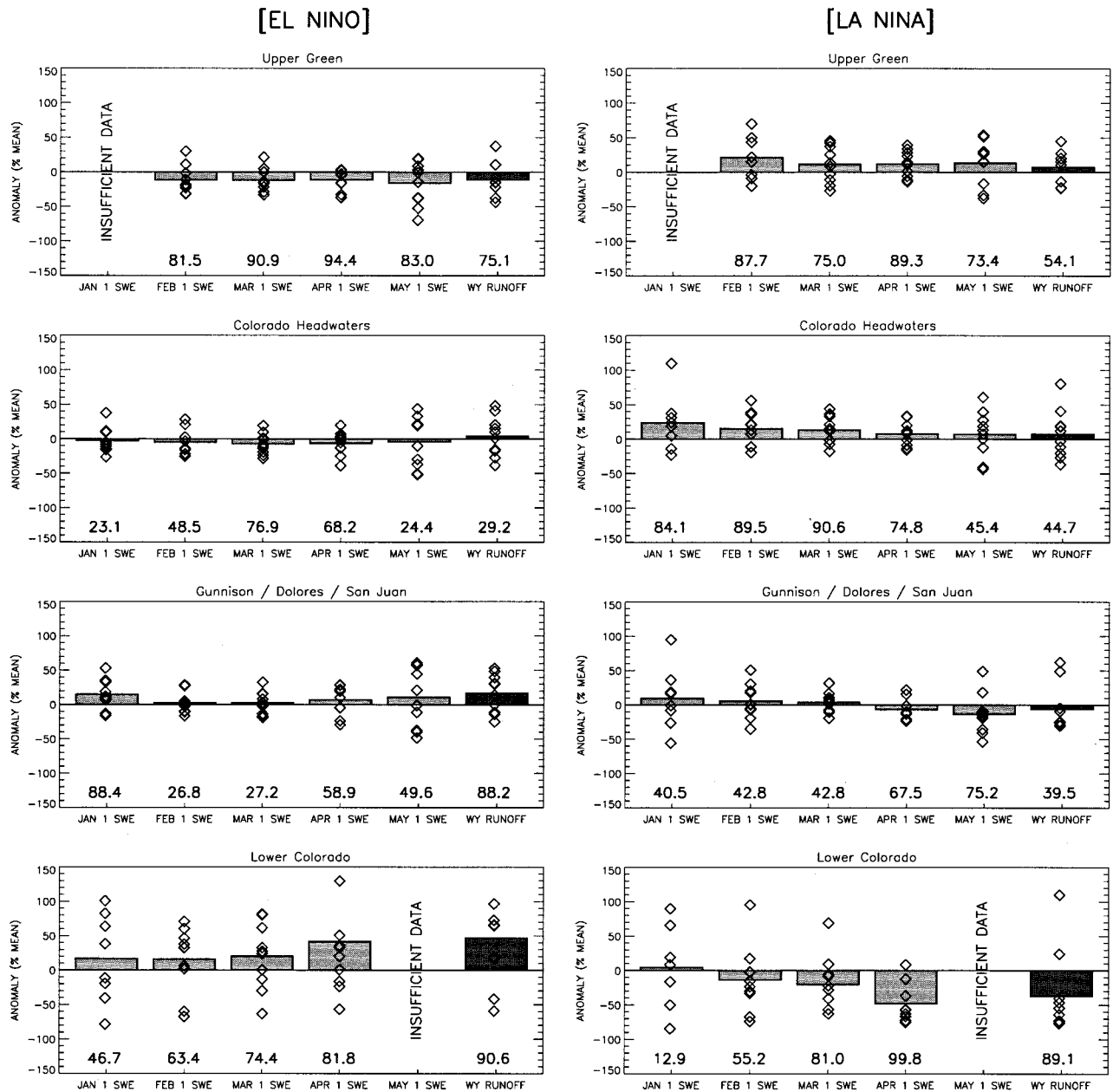


Figure 8. Anomalous monthly SWE and annual runoff (expressed as a percentage of the mean) in El Niño and La Niña years for the major subbasins in the Colorado River Basin. The bars represent the composite mean of the 10 strongest El Niño and La Niña years (based on the Niño 3.4 index, Table 4), and the diamonds represent the individual composite members. The April 1 SWE in the Lower Colorado in the 1972/1973 El Niño event is off the scale at 216% of the mean (not plotted). Significance estimates (in percent) based on t tests are displayed on the bottom of each plot.

anomalies for all other El Niño and La Niña years. Such predictions of runoff can be made in autumn before any snow has accumulated.

2. In the persistence scheme, SWE anomalies at various points in the accumulation season are used to predict runoff for the remainder of the water year (e.g., for predictions based on January 1 SWE, runoff for the rest of the water year would be for the period January 1 through September 30). Since most of the annual runoff in snowmelt-dominated river basins occurs during May and June (Figures 4 and 5), runoff forecasts based on the midwinter snowpack are made several months in advance. These predictions take the form

$$R_{\text{PRED}} = (Z_{\text{SWE}} * \sigma_R) + \mu_R, \quad (1)$$

where R_{PRED} is the predicted runoff, Z_{SWE} is the SWE (e.g., on January 1) expressed as a z score, σ_R is the standard deviation of the runoff time series, and μ_R is the mean of the runoff time series. Note that some of the variability of SWE in these persistence forecasts is accounted for by ENSO.

3. In the persistence and ENSO scheme, runoff anomalies in a given El Niño or La Niña year are equal to the normalized SWE anomalies at a given point in the accumulation season (e.g., January 1) plus the difference between the mean SWE in ENSO years for the date of the forecast (in this case, this

Table 6. Mean Anomalous SWE and Annual Runoff for the Colorado River Basin^a

	Variable	Nino 3.4 Years in Composite					SOI Years in Composite				
		6	8	10	12	14	6	8	10	12	14
<i>El Nino</i>											
Upper Green	Jan. 1 SWE	ND	ND	ND	ND	ND	ND	ND	ND	ND	ND
	Feb. 1 SWE	-17.94	-11.95	-11.62	-16.37	-14.36	-4.58	-5.20	-6.78	-4.32	-11.74
	March 1 SWE	-17.36	-12.26	-12.00	-17.63	-12.20	-8.35	-8.29	-6.09	-4.47	-9.04
	April 1 SWE	-16.14	-12.02	-11.61	-15.03	-8.83	-10.29	-10.11	-6.90	-5.71	-9.51
	May 1 SWE	-22.89	-17.88	-16.14	-19.66	-17.84	-15.74	-17.15	-14.92	-12.78	-19.01
	Annual runoff	-9.90	-6.96	-11.21	-14.21	-12.39	-3.97	-7.03	-7.23	-5.27	-7.95
Colorado Headwaters	Jan. 1 SWE	-4.09	-7.84	-2.48	-12.41	-12.76	1.87	1.93	3.08	-0.74	-5.22
	Feb. 1 SWE	-12.94	-9.86	-4.81	-12.25	-4.76	-5.87	-7.81	0.32	0.20	-5.19
	March 1 SWE	-16.13	-11.88	-7.45	-13.70	-6.34	-6.08	-7.85	-2.48	-1.93	-6.45
	April 1 SWE	-13.15	-10.75	-6.43	-10.67	-3.61	-3.95	-4.92	-0.22	-0.80	-4.91
	May 1 SWE	-10.94	-9.20	-3.96	-8.23	-2.57	-6.40	-6.10	0.22	-0.56	-7.13
	Annual runoff	-1.11	4.47	3.89	-3.64	0.86	2.83	-1.45	4.83	7.63	1.23
San Juan	Jan. 1 SWE	26.65	19.19	14.77	0.29	-1.89	11.37	0.99	6.91	5.21	-0.20
	Feb. 1 SWE	0.79	4.56	2.43	-7.59	2.29	2.51	-6.03	8.08	9.31	1.45
	March 1 SWE	3.35	7.54	2.44	-8.09	2.03	10.40	2.94	11.67	12.96	5.99
	April 1 SWE	8.53	12.79	6.82	-2.34	7.33	12.05	6.05	14.27	16.04	9.00
	May 1 SWE	11.32	15.49	10.52	1.67	11.28	5.64	4.07	15.99	17.80	9.25
	Annual runoff	20.69	22.14	16.62	6.89	10.44	14.39	10.20	16.44	18.16	11.51
Lower Colorado	Jan. 1 SWE	ND	37.48	16.87	ND	ND	ND	ND	ND	ND	5.38
	Feb. 1 SWE	23.77	24.41	16.05	6.05	12.43	42.44	17.30	23.43	24.34	10.98
	March 1 SWE	41.70	34.76	20.16	8.09	15.48	57.92	35.59	39.82	35.70	24.57
	April 1 SWE	79.08	60.84	41.36	29.49	39.29	39.82	26.33	53.48	45.60	32.91
	May 1 SWE	ND	ND	ND	ND	ND	ND	ND	ND	ND	ND
	Annual runoff	80.60	63.48	46.54	29.47	31.63	78.18	53.56	66.22	56.94	40.55
<i>La Nina</i>											
Upper Green	Jan. 1 SWE	ND	ND	ND	ND	ND	ND	ND	ND	ND	ND
	Feb. 1 SWE	21.43	24.58	21.05	13.48	20.11	30.61	23.79	7.74	6.33	7.68
	March 1 SWE	12.35	9.06	11.22	7.84	14.94	23.34	17.68	8.09	4.48	4.83
	April 1 SWE	12.21	10.57	11.91	8.69	12.93	19.98	14.36	6.21	4.26	4.70
	May 1 SWE	9.50	8.38	13.33	14.43	19.69	23.23	21.28	13.50	12.79	11.84
	Annual runoff	9.25	4.75	7.54	6.83	14.86	13.45	14.12	6.28	3.89	4.87
Colorado Headwaters	Jan. 1 SWE	10.07	11.29	23.59	19.44	21.33	7.35	-2.44	-9.57	-8.77	-0.87
	Feb. 1 SWE	10.64	10.39	15.26	12.84	13.63	11.86	7.32	-1.23	-2.14	1.41
	March 1 SWE	9.81	10.65	13.35	12.04	13.68	12.44	10.48	3.90	2.30	2.84
	April 1 SWE	2.01	4.01	7.68	7.05	9.04	4.03	-0.20	-3.72	-3.08	-1.77
	May 1 SWE	-0.73	-1.03	7.15	9.27	11.28	1.83	-2.60	-9.75	-10.02	-7.25
	Annual runoff	0.69	-0.50	7.35	7.39	11.31	-6.27	-8.10	-11.38	-10.66	-4.76
San Juan	Jan. 1 SWE	5.92	-2.87	9.36	8.70	14.34	0.67	5.97	-0.18	-0.28	2.90
	Feb. 1 SWE	7.36	1.30	5.43	5.27	7.70	2.49	3.75	-2.66	-4.52	-1.19
	March 1 SWE	5.62	1.97	3.72	5.20	7.06	2.10	-0.42	-3.41	-3.46	-2.16
	April 1 SWE	-7.15	-8.45	-6.68	-2.22	0.39	-13.71	-17.98	-16.54	-12.93	-8.71
	May 1 SWE	-18.33	-20.73	-13.59	-1.70	2.36	-25.18	-30.06	-31.29	-23.21	-17.91
	Annual runoff	-9.84	-12.29	-6.20	-3.82	1.75	-22.11	-24.59	-24.01	-21.04	-13.98
Lower Colorado	Jan. 1 SWE	21.51	3.85	4.49	20.55	13.77	ND	ND	ND	ND	ND
	Feb. 1 SWE	0.62	-9.03	-13.55	0.99	-4.12	-19.18	-29.03	-19.37	-18.45	-7.64
	March 1 SWE	-7.89	-14.82	-20.33	-10.00	-10.93	-23.32	-34.92	-23.91	-20.53	-10.91
	April 1 SWE	-39.58	-44.67	-48.16	-31.54	-30.30	-50.52	-52.02	-48.86	-42.66	-34.25
	May 1 SWE	ND	ND	ND	ND	ND	ND	ND	ND	ND	ND
	Annual runoff	-35.17	-40.20	-37.14	-26.08	-23.41	-66.24	-58.26	-50.14	-46.46	-33.75

^aComputed using the (x) strongest El Nino years and the (x) strongest La Nina years (Table 4) for the Nino 3.4 index and the SOI. Composites are tabulated if at least 70% of the years hold valid data (ND indicates insufficient data). Values are given as percent of the mean.

would be the January 1 SWE signal) and the mean runoff in ENSO years (in this case, the January 1 through September 30 runoff signal). This scenario thus includes information on seasonal changes in ENSO associations. These predictions take the form

$$R_{\text{PRED}} = \{[Z_{\text{SWE}} + (Z_{\text{R_ENSO}} - Z_{\text{SWE_ENSO}})] * \sigma_{\text{R}}\} + \mu_{\text{R}} \quad (2)$$

where R_{PRED} is the predicted runoff, Z_{SWE} is the SWE (e.g., on January 1) expressed as a z score, $Z_{\text{R_ENSO}}$ is the ENSO runoff association expressed as a z score, $Z_{\text{SWE_ENSO}}$ is the ENSO SWE association expressed as a z score. As before, σ_{R} is the standard deviation of the runoff time series, and μ_{R} is the mean of the runoff time series.

In scenarios 1 and 3 the predicted year is not included in computations of the mean El Nino and La Nina anomalies (i.e., the means are based on nine cases). Implicit in these predictive scenarios is a perfect forecast of the ENSO state (see section 5.1). We employ as the measure of error the mean absolute error, which, for all three scenarios, is computed using only the 10 El Nino and La Nina years. The skill score [Wilks, 1995] is used to assess the skill of the runoff predictions with respect to predictions based on mean value of the runoff time series. The skill score (SS) takes the form

$$\text{SS} = \left(1 - \frac{\text{MAE}_{\text{PRED}}}{\text{MAE}_{\text{CLIM}}}\right) 100. \quad (3)$$

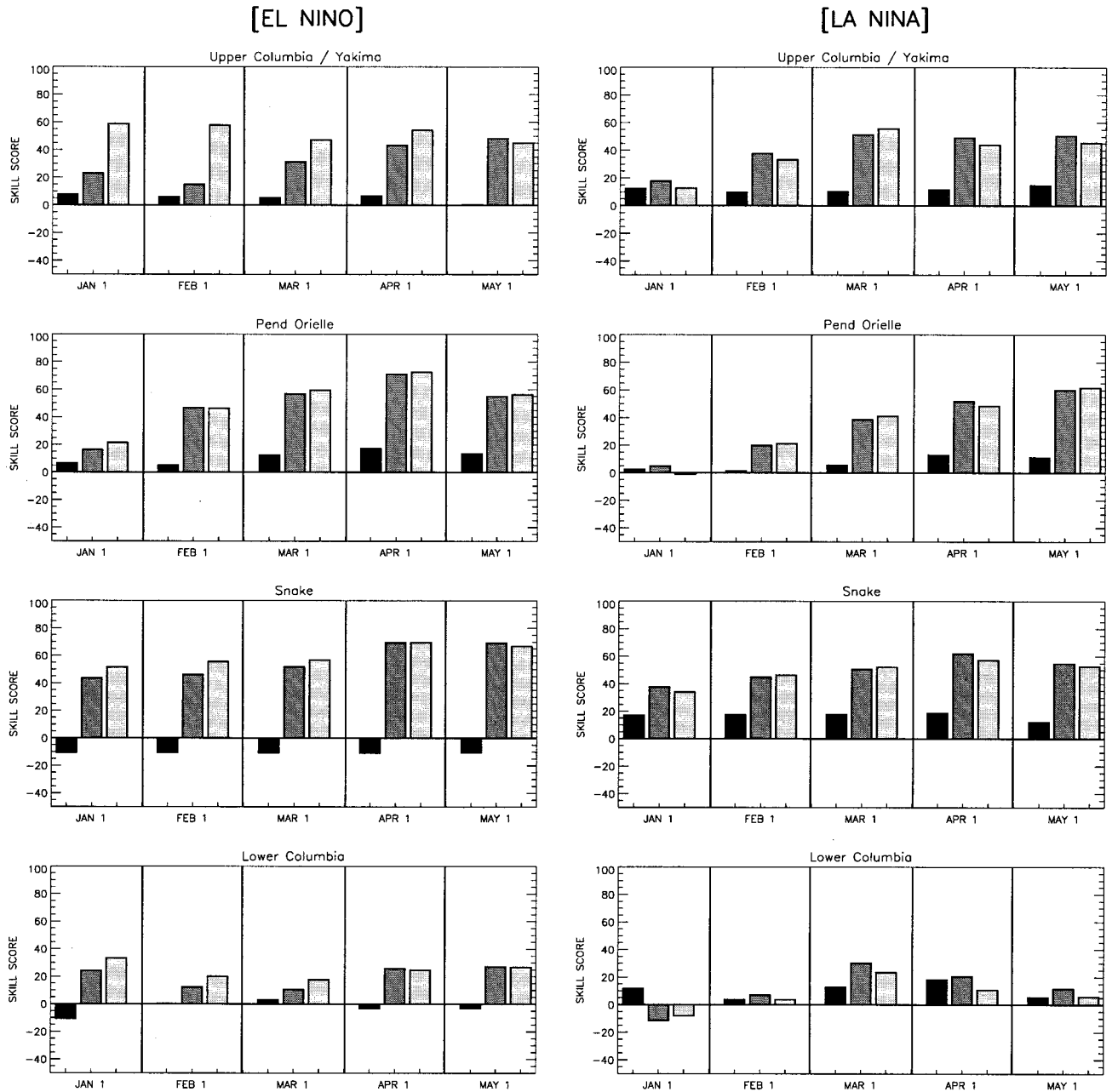


Figure 9. Skill scores for the three runoff prediction schemes outlined in the text for subbasins in the Columbia River system. Dark shaded bars illustrate forecast improvement upon climatology using only ENSO information, medium shaded bars illustrate forecast skill improvement using the amount of water stored in the seasonal snowpack (persistence), and light shaded bars illustrate forecast skill improvement combining the seasonal change in ENSO associations with persistence. Predictions of runoff for the rest of the water year are made on January 1, February 1, March 1, April 1, and May 1.

Here MAE_{PRED} is the mean absolute error (MAE) of the predicted runoff, and MAE_{CLIM} is the MAE of predictions based on climatology. Climatology in this case is mean runoff for the period of the prediction (i.e., for January 1 predictions, MAE_{CLIM} would be computed using as the predictor mean runoff from January 1 through September 30). Equation (3) expresses the percent improvement of the forecasts over those based on climatology. With only 10 El Niño and La Niña years our results are sensitive to the small sample size and should be taken as preliminary until they can be validated in an independent experiment. While categorical, rather than deterministic,

measures of forecast skill are often more useful for decision making, the small number of El Niño and La Niña years in our time series precludes a categorical analysis.

Results from the three predictive experiments are summarized for the Columbia River Basin in Figure 9. Using only ENSO information, improvements in forecast skill over climatology are apparent in the Upper Columbia/Yakima and Pend Orielle River Basins for El Niño years and, to varying degrees, in all four river basins for La Niña years. Given an accurate prediction of the November–April ENSO state, these predictions may be realized up to 9 months in advance. Predictions

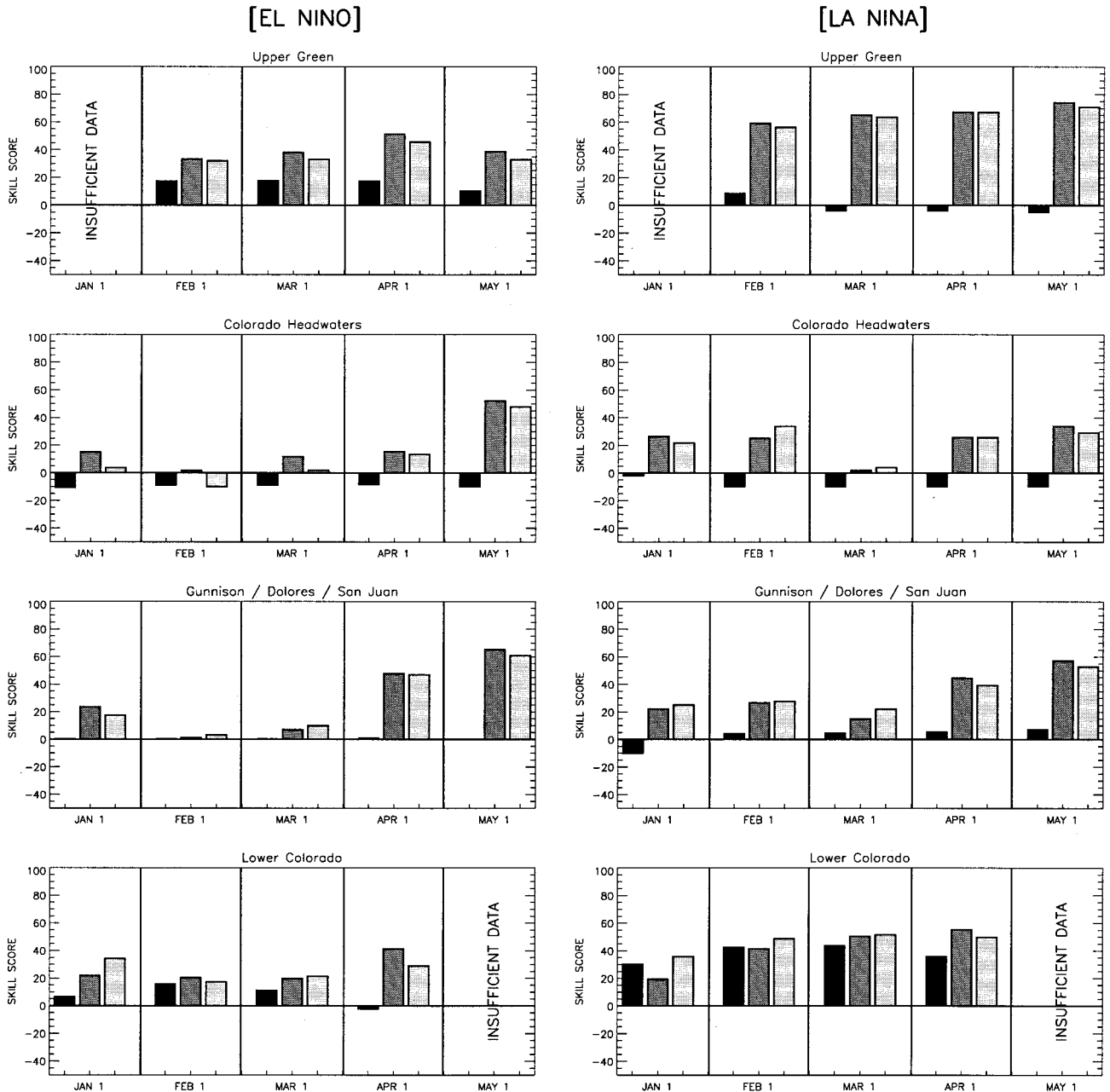


Figure 10. Skill scores for the three runoff prediction schemes outlined in the text for subbasins in the Colorado River system. Dark shaded bars illustrate forecast improvement upon climatology using only ENSO information, medium shaded bars illustrate forecast skill improvement using the amount of water stored in the seasonal snowpack (persistence), and light shaded bars illustrate forecast skill improvement combining the seasonal change in ENSO associations with persistence. Predictions of runoff for the rest of the water year are made on January 1, February 1, March 1, April 1, and May 1.

based on persistence are, in almost all cases, of greater skill than those based on ENSO information alone. This is expected given the correlations presented in Table 3. These results simply show that even in midwinter, much of the spring runoff is already stored in the snowpack. Of particular interest in Figure 9 is the predictive skill realized when seasonal changes in ENSO associations are combined with knowledge of the water equivalent of the seasonal snowpack. In most basins in the Columbia River system, seasonal changes in ENSO associations are minimal (Figure 7), and the predictive skill from the combined scenario provides no improvement, or only a small improvement, over persistence. However, in basins where sea-

sonal changes in the ENSO association are large (e.g., the Upper Columbia/Yakima in El Niño years), significant improvements in forecast skill are realized. Note also the smaller improvements over persistence in the Snake and Lower Columbia River Basins, where seasonal changes in El Niño associations are still present, albeit more subdued.

For the Colorado River Basin, predictions using only ENSO information provide a small improvement in skill over climatology in the Upper Green (for El Niño years) and the Lower Colorado River Basin (for both El Niño and La Niño years) (Figure 10). In the Lower Colorado, improvements in skill using ENSO only are more pronounced for La Niño years as

inter-ENSO variability is lower. In most cases, predictions based on persistence are more skillful than those using only ENSO information. However, forecast skill using persistence is rather low in the Colorado Headwaters and the Gunnison/Dolores/San Juan River Basins in midwinter and early spring for El Niño years, and in March for La Niña years. Furthermore, persistence is less skillful than ENSO-based predictions in the Lower Colorado for January and February. Combining seasonal changes in the ENSO association with persistence provides little improvement over persistence alone in most subbasins in the Colorado River system. Improvements in forecast skill, however, are apparent for the Lower Colorado River system in January for El Niño years and in both January and February for La Niña years. This is in line with the large seasonal changes in ENSO associations in the southwestern United States. Also of note are the small improvements in forecast skill over persistence in the Colorado Headwaters in February for La Niña years. The Colorado region is typically regarded as being the midpoint of a see-saw with moderately strong opposing ENSO associations to the north and south but no associations in Colorado itself (in the April 1 SWE composites of *Cayan* [1996] the zero line cuts directly through Colorado). While it appears that these seasonal changes provide at least some benefit in our simple predictive model, it should be kept in mind that the midwinter increases in SWE in these basins are not evident when the Niño 3.4 index is replaced with the SOI (Table 6). Further research is necessary to quantify the reliability of such associations.

6. Summary and Conclusions

Monthly snow-water equivalent (SWE) and stream flow data measured at several hundred sites over the western United States are used to examine the historic effects of El Niño and La Niña events on the seasonal evolution of snowpack in the major subbasins in the Columbia and Colorado River systems. The results were used to predict runoff.

To first order, our results mirror those in other studies [e.g., *Cayan and Webb*, 1992]. El Niño (La Niña) events lead to decreased (increased) SWE and annual runoff in the Pacific Northwest, and increased (decreased) SWE and annual runoff over the desert southwest. However, additional information is provided by examining seasonal changes in these signals. In the Columbia River Basin it is found that the negative anomalies in SWE during El Niño years are much less pronounced than the corresponding positive anomalies in La Niña years and, for the most part, are not statistically significant. This lack of symmetry between El Niño and La Niña years is most evident in basins nearest the Pacific coast (the Upper and Lower Columbia) and occurs because midwinter SWE anomalies in El Niño years are actually positive. These midwinter increases occur in conjunction with an eastward shift of the Aleutian Low in El Niño years [*Hoerling and Kumar*, 2000], and largely cancel out the expected seasonal decreases in SWE [see also *Livezey et al.*, 1997].

Similar seasonalities are found in the Colorado River Basin. Here mean changes in SWE and annual runoff during El Niño years depict a transition between drier-than-average conditions in the north and wetter-than-average conditions in the southwest. La Niña signals are generally opposing. However, anomalies in SWE in the Lower Colorado tend to be much more pronounced in spring than in midwinter. There is some evidence of similar but weaker seasonal changes in the Colo-

rado Headwaters and the Gunnison, Dolores, and San Juan River Basins. These associations occur in part because the precipitation anomalies over the southwest associated with changes in the intensity of the subtropical jet are most pronounced in spring. Sensitivity tests show that while ENSO associations in the Upper Green and Lower Colorado are fairly robust, those in the Colorado Headwaters and the San Juan River Basin are sensitive to both the number of years included in the El Niño and La Niña composites and the type of index used.

Cross-validated prediction experiments reveal that in some basins there is modest skill in predicting runoff using only ENSO information. For El Niño years this is most apparent in the Upper Columbia/Yakima, the Pend-Orielle, the Upper Green, and the Lower Colorado River Basins. For La Niña years, modest skill is apparent in the Upper Columbia/Yakima, the Pend-Orielle, the Snake, the Lower Columbia, and the Lower Colorado River Basins. Given accurate predictions of the ENSO state, these hydrologic forecasts can be made in autumn before any snow has accumulated. Predictions based on the water stored in the midwinter snowpack are, in almost all cases, much higher than those based on ENSO information alone. This occurs because much of the spring runoff is already stored in the snowpack in midwinter. Since many water management decisions are made in the middle of winter, the challenge is to identify ways in which one can improve upon persistence-based forecasts. Our results suggest that combining the seasonal changes in ENSO associations with persistence leads to improved streamflow predictions in basins where the seasonal changes in ENSO associations are strong. The most notable improvements are found in the Upper Columbia/Yakima River Basin in El Niño years and in the Lower Colorado River Basin in both El Niño and La Niña years. Smaller improvements in forecast skill are apparent in the Colorado Headwaters where ENSO associations have traditionally been perceived as nonexistent.

Acknowledgments. This work was funded by NSF grants EAR-9634329 and ATM-9900687, NASA grant NAG13-99005, and the NOAA Regional Assessment Program (NOAA Cooperative Agreement NA67RJ0153). Comments from Richard Armstrong, Allan Frei, and Klaus Wolter are also appreciated.

References

- Bjerknes, J., Atmospheric teleconnections from the equatorial Pacific, *Mon. Weather Rev.*, **97**, 163–172, 1969.
- Cayan, D. R., Interannual climate variability and snowpack in the western United States, *J. Clim.*, **9**, 928–948, 1996.
- Cayan, D. R., and D. H. Peterson, The influence of North Pacific circulation on streamflow in the west, in *Aspects of Climate Variability in the Pacific and Western Americas*, *Geophys. Monogr. Ser.*, vol. 55, edited by D. H. Peterson, pp. 375–398, AGU, Washington, D. C., 1990.
- Cayan, D. R., and R. H. Webb, El Niño/Southern Oscillation and streamflow in the western United States, in *El Niño: Historical and Paleoclimatic Aspects of the Southern Oscillation*, edited by H. Diaz and V. Markgraf, pp. 29–68, Cambridge Univ. Press, New York, 1992.
- Cayan, D. R., K. T. Redmond, and L. G. Riddle, ENSO and hydrologic extremes in the western United States, *J. Clim.*, **12**, 2881–2893, 1999.
- Chen, D., S. E. Zebiak, M. A. Cane, and A. J. Busalacchi, Initialization and predictability of a coupled ENSO forecast model, *Mon. Weather Rev.*, **125**, 773–788, 1997.
- el-Ashry, M., and D. Gibbons, *Water and Arid Lands of the Western United States*, Cambridge Univ. Press, New York, 1988.

- Hoerling, M. P., and A. Kumar, Understanding and predicting extratropical teleconnections related to ENSO, in *El Niño and the Southern Oscillation: Multiscale Variability and Global and Regional Impacts*, edited by H. F. Diaz and V. Markgraf, Cambridge Univ. Press, New York, in press, 2000.
- Hoerling, M. P., A. Kumar, and M. Zhong, El Niño, La Niña, and the nonlinearity of their teleconnections, *J. Clim.*, *10*, 1769–1786, 1997.
- Horel, J. D., and J. M. Wallace, Planetary scale atmospheric phenomena associated with the Southern Oscillation, *Mon. Weather Rev.*, *109*, 813–829, 1981.
- Ji, M., A. Kumar, and A. Leetmaa, A multiseason climate forecast system at the National Meteorological Center, *Bull. Am. Meteorol. Soc.*, *75*, 569–577, 1994.
- Ji, M., D. W. Behringer, and A. Leetmaa, An improved coupled model for ENSO prediction and implications for ocean initialization, part II, The coupled model, *Mon. Weather Rev.*, *126*, 1022–1034, 1998.
- Koch, R. W., C. F. Buzzard, and D. M. Johnson, Variation of snow water equivalent and streamflow in relation to the El Niño/Southern Oscillation, paper presented at 19th Annual Meeting of the Western Snow Conference, Juneau, Alaska, April 12–15, 1991.
- Kohler, M. A., T. J. Nordenson, and D. R. Baker, Evaporation maps for the United States, *Tech. Pap. 37*, U.S. Weather Bur., Washington, D. C., 1959.
- Livezey, R. E., M. Masutani, A. Leetmaa, H. Rui, M. Ji, and A. Kumar, Teleconnective response of the Pacific-North American region atmosphere to large central equatorial Pacific SST anomalies, *J. Clim.*, *10*, 1787–1820, 1997.
- McCabe, G. J., and M. D. Dettinger, Decadal variations in the strength of ENSO teleconnections with precipitation in the western United States, *Int. J. Climatol.*, *19*, 1399–1410, 1999.
- Natural Resources Conservation Service (NRCS), Snow surveys and water supply forecasting, *Agric. Inf. Bull. U.S. Dep. Agric.*, *536*, 1988.
- Panofsky, H. A., and G. W. Brier, *Some Applications of Statistics to Meteorology*, 224 pp., Pa. State Univ., University Park, 1968.
- Penland, C., and T. Magorian, Prediction of Niño 3 sea surface temperatures using linear inverse modeling, *J. Clim.*, *6*, 1067–1076, 1993.
- Pulwarty, R. S., and K. Redmond, The role of climate forecasts in the management of salmon and hydropower in the Columbia River Basin, *Bull. Am. Meteorol. Soc.*, *78*, 381–397, 1997.
- Rasmusson, E. M., and J. M. Wallace, Meteorological aspects of the El Niño/Southern Oscillation, *Science*, *222*, 1195–1202, 1983.
- Redmond, K. T., and R. W. Koch, Surface climate and streamflow variability in the western United States and their relationship to large-scale circulation indices, *Water Resour. Res.*, *27*, 2381–2399, 1991.
- Rhodes, S. L., D. Ely, and J. A. Dracup, Climate and the Colorado River: The limits of management, *Bull. Am. Meteorol. Soc.*, *65*, 682–691, 1984.
- Seaber, P. R., F. P. Kapinos, and G. L. Knapp, Hydrologic unit maps, *U.S. Geol. Surv. Water Supply Pap.*, *2294*, 63 pp., 1987.
- Serreze, M. C., M. P. Clark, R. L. Armstrong, D. A. McGinnis, and R. S. Pulwarty, Characteristics of the western U.S. snowpack from snowpack telemetry (SNOTEL) data, *Water Resour. Res.*, *35*, 2145–2160, 1999.
- Slack, J. R., and J. M. Landwehr, Hydro-Climatic Data Network (HCDN): A U.S. Geological Survey streamflow data set for the United States for the study of climate variations, 1874–1988, *U.S. Geol. Surv. Open File Rep.*, *92-129*, 200 pp., 1992.
- Trenberth, K. E., The definition of El Niño, *Bull. Am. Meteorol. Soc.*, *78*, 2771–2777, 1997.
- Wilks, D. S., *Statistical Methods in the Atmospheric Sciences: An Introduction*, 467 pp., Academic, San Diego, Calif., 1995.
- Wolter, K., R. M. Dole, and C. A. Smith, Short-term climate extremes over the continental U.S. and ENSO, part I, Seasonal temperatures, *J. Clim.*, *12*, 3255–3272, 1999.
-
- M. P. Clark and M. C. Serreze, Cooperative Institute for Research in Environmental Sciences, University of Colorado, Boulder, CO 80309-0449. (clark@vorticity.colorado.edu; serreze@coriolis.colorado.edu)
- G. J. McCabe, U.S. Geological Survey, P.O. Box 25046, MS 412, Denver Federal Center, Lakewood, CO 80225-0046. (gmccabe@usgs.gov)

(Received April 9, 1999; revised March 27, 2000; accepted September 28, 2000.)

